

Coulomb excitation of ground bands in $^{160, 162, 164}\text{Dy}$ with ^{20}Ne and ^{35}Cl ions*

R. O. Sayer

*Furman University, Greenville, South Carolina 29613,
and Oak Ridge National Laboratory, Oak Ridge, Tennessee 37830*

and

E. Eichler, Noah R. Johnson, and D. C. Hensley

Oak Ridge National Laboratory, Oak Ridge, Tennessee 37830

and

L. L. Riedinger

University of Tennessee, Knoxville, Tennessee 37916

(Received 17 September 1973)

Multiple Coulomb excitation of states up to $J^\pi = 12^+$ in the ground band was measured to test the rigid-rotor prediction for intraband $B(E2)$ ratios. The deexcitation γ rays were observed in singles and in the particle- γ coincident mode following excitation by ^{20}Ne or ^{35}Cl ions from the Oak Ridge isochronous cyclotron. $B(E2)$ values were extracted by comparing experimental excitation probabilities with theoretical values calculated with the Winther-de Boer computer code. An unexpected result is that the $B(E2; 4 \rightarrow 6)$ values for $^{162, 164}\text{Dy}$ are $15 \pm 5\%$ smaller than the rotational values. However, the most striking variation of $B(E2)$ with spin occurs for ^{160}Dy . We find $B(E2)_{\text{exp}}/B(E2)_{\text{rotational}} = 0.77 \pm 0.05$, 0.94 ± 0.06 , and 1.29 ± 0.14 for the $4 \rightarrow 6$, $6 \rightarrow 8$, and $8 \rightarrow 10$ transitions, respectively. The $10 \rightarrow 8$ transition in ^{160}Dy is significantly faster than rotational even when our approximate quantal correction of 6% is not included in the analysis.

[NUCLEAR REACTIONS $^{160, 162, 164}\text{Dy}(^{35}\text{Cl}, ^{35}\text{Cl}')$, $E = 125$ MeV; $(^{20}\text{Ne}, ^{20}\text{Ne}')$,
 $E = 72$ MeV; measured Coulomb excitation yields. $^{160, 162, 164}\text{Dy}$ levels, deduced
 E_γ , $B(E2)$.]

I. INTRODUCTION

The energy spacings of levels in the ground-state bands of even-even rare-earth nuclei have received extensive experimental and theoretical investigation. One quality index for rotational nuclei is the ratio B/A obtained by a fit of the first four or five level energies to the expansion $E(I) = AI(I+1) - BI^2(I+1)^2 + \dots$. If $B/A \approx 10^{-3}$ one may characterize the nucleus as a "good rotor" in contrast to a "soft rotor" for which $B/A \approx 10^{-2}$. A recent phenomenological treatment, the variable moment of inertia (VMI) model,¹ gives an excellent fit of the level energies up to spin 12 or 14 for both good and poor rotors, whereas the power-series expansion is generally inadequate for $I > 8$.

The observed small departures from the $I(I+1)$ rule may be manifestations of interesting changes in the intrinsic nuclear structure. The nature of these changes is still not clear, although several mechanisms have been proposed to account for the observed increase in nuclear moment of inertia with increasing spin. A number of theoretical cal-

culations based on microscopic models² indicate that centrifugal stretching, Coriolis antipairing, and fourth-order cranking-model corrections are probably the most important factors which depress the energy levels.

The aforementioned factors should cause the intraband $B(E2)$ values to deviate from the predictions of a rigid rotor. Unfortunately, we can relate the deviations in level energies to deviations in $B(E2)$ values only for the centrifugal stretching effect. For a good rotor this procedure yields predicted increases in $B(E2)$ values relative to rotational of 3, 6, and 10% for the $4 \rightarrow 6$, $6 \rightarrow 8$, and $8 \rightarrow 10$ transitions, respectively. Although $B(E2; 4 \rightarrow 6)$ and $B(E2; 6 \rightarrow 8)$ values were reported³ as early as 10 years ago, only recently have experimental accuracies approached the magnitudes of possible deviations. Accurate $B(E2; 6 \rightarrow 8)$ and $B(E2; 4 \rightarrow 6)$ values for good rotors have been measured by Sayer *et al.*⁴ (^{168}Er , $^{172, 4, 6}\text{Yb}$), Diamond *et al.*² (^{154}Sm), and Riedinger *et al.*⁵ ($^{168-176}\text{Yb}$). Ward *et al.*⁶ recently measured $B(E2; 2 \rightarrow 4)$ and $B(E2; 4 \rightarrow 6)$ values for ^{156}Gd . The experimental $B(E2)$ val-

ues for these good rotors are not significantly larger than the rotational predictions. Diamond *et al.*⁷ used the recoil-distance lifetime technique to obtain $B(E2; 8-10)/B(E2)_{\text{rotational}} = 0.75 \pm 0.29$ for the poor rotor ^{160}Er , but no $B(E2)$ values for $I > 8$ for good rotors had been reported prior to the present work.

It seemed important to us to perform accurate $B(E2)$ measurements above spin 8 to provide an even more stringent test of the rotational model and possibly to elucidate the relative importance of proposed perturbing influences. We report herein the results of Coulomb excitation measurements on three Dy nuclei with ^{20}Ne and ^{35}Cl ions.⁸ The nuclei $^{162,164}\text{Dy}$ were selected for their low-lying ground bands and small B/A values, and the nucleus ^{160}Dy provides a case for study of transition probabilities in a nucleus with known back-bending behavior of the moment of inertia.⁹ The availability of an energetic ^{35}Cl beam was crucial in the achievement of the experimental sensitivity necessary for accurate measurement of excitation probabilities for the 10^+ states.

II. EXPERIMENTAL METHOD

Multiple Coulomb excitation was produced by 72-MeV ^{20}Ne ions and 125-MeV ^{35}Cl ions from the Oak Ridge isochronous cyclotron. The targets were foils of 40–50-mg/cm² thickness fabricated from enriched isotopic material. A 40-cm³ Ge(Li) detector was used to observe the deexcitation γ rays in singles and in coincidence with heavy ions backscattered into a ring counter which subtended an angular range of either 164°–175° or 151°–171° in the laboratory. Most of the data were taken with the targets inclined 45° relative to the incident beam direction and with the Ge(Li) detector at 90° since Doppler broadening was observed for the faster transitions. However, several measurements were made with γ -ray counters at 0 and 55°.

Three parameter coincident data for the HI- γ coincident measurements consisted of the γ -ray energy, the backscattered HI energy, and the coincident time correlation from a time-to-amplitude converter. These parameters were digitized in a fast analog-to-digital converter, filed on disc, and subsequently copied onto magnetic tape.

Since gating restrictions were placed on the HI energy spectra in the analysis of data, it was necessary to determine the energy response of the ring counter in order to compute the effective target thickness in MeV. This was done by acquiring backscattered HI spectra from several targets of different atomic weight. A typical effective target thickness was 20 MeV for ^{35}Cl .

Only the efficiency of the Ge(Li) detector for one

γ ray relative to another is needed to determine $B(E2)$ values from ratios of excitation probabilities. This relative efficiency was measured to an accuracy of 3% or better for the energy range of interest, 150–600 keV, by using ^{226}Ra and ^{182}Ta sources and the relative intensities of Gunnick *et al.*¹⁰ and Jardine.¹¹ A cross calibration with absolute International Atomic Energy Agency standards yielded absolute efficiencies accurate to 5%.

III. EXPERIMENTAL RESULTS

Transition rates were extracted from ^{35}Cl - γ coincident yields and from thick-target γ -ray yields. Table I contains a summary of the observed ground-band states and the internal-conversion coefficients, α_T . In this work the large α_T values for the 2–0 transitions were not used since we did not determine $B(E2; 0-2)$ values.¹²

The 10^+ and 12^+ levels in $^{162,164}\text{Dy}$ had not been observed prior to this work. However, Hagemann *et al.*¹³ recently populated states up to spin 12 in ^{164}Dy by inelastic scattering of 153-MeV ^{40}Ar ions. Their energies of 342.3, 417.4, and 484.2 keV for the 8–6, 10–8, and 12–10 transitions, respectively, are in good agreement with our values. All other states given in Table I had been established previously.^{9,14–16}

TABLE I. Summary of rotational states in $^{160,162,164}\text{Dy}$ observed by Coulomb excitation. In column 6, we list the values for the total internal-conversion coefficients used for the γ -ray transitions given in column 4.

Nucleus	Level (keV)	J	E_γ (keV)	J_f	α_T
^{160}Dy	86.79	2	86.79 ^a	0	4.75
	283.79	4	197.00 ± 0.07	2	0.250
	581.03	6	297.24 ± 0.08	4	0.067
	966.71	8	385.68 ± 0.10	6	0.031
	1428.59	10	461.88 ± 0.13	8	0.019
	1951.4	12	522.8 ^b	10	0.014
^{162}Dy	80.660	2	80.660 ^c	0	6.24
	265.665	4	185.005 ^c	2	0.311
	548.53	6	282.86 ± 0.06	4	0.078
	921.28	8	372.75 ± 0.08	6	0.035
	1375.13	10	453.85 ± 0.09	8	0.018
	1903.0	12	528.0 ± 2.0	10	0.013
^{164}Dy	73.39	2	73.39 ^d	0	9.08
	242.23	4	168.84 ^d	2	0.426
	501.32	6	259.09 ^d	4	0.103
	843.67	8	342.35 ± 0.07	6	0.044
	1261.3	10	417.6 ± 0.2	8	0.025
	1745.3	12	484.0 ± 1.0	10	0.016

^a Reference 14.

^c Reference 15.

^b Reference 9.

^d Reference 16.

A. Thick target yields

We performed γ -ray yield measurements because quantum-mechanical corrections to the Coulomb excitation theory are expected to be smaller than in the case of backscatter particle- γ coincident yields and because the quality of agreement between values obtained by singles and by particle- γ measurements was a useful check on some of the data analysis procedures.

Singles γ -ray spectra were taken following Coulomb excitation of $^{162,164}\text{Dy}$ with 72.8-MeV ^{20}Ne ions and with ^{35}Cl ions of incident energies 126.5 and 127.6 MeV. A representative γ -ray spectrum is shown in Fig. 1. The 8-6 γ ray is relatively intense but the 10-8 γ ray is weak. The procedure for computation of experimental yields has been discussed previously.⁴ In the analysis particular care was taken to include in the peak areas tails arising from Doppler-shifted γ rays and counts lost to true coincident summing.

Theoretical yields were calculated with the Winther-de Boer computer program for E_1 , E_2 , E_3 , and E_4 excitation¹⁷ suitably modified to perform integration over projectile energy and scattering angle. The yield Y_J for the state of spin J is given by

$$Y_J = \frac{3.76 \times 10^{33}}{qA_2'} \int_0^{E_i} \frac{\sigma_J(E)}{S(E)} dE \quad (1)$$

in units of excitations per microcoulomb. Here q is the projectile charge state, A_2' is the atomic weight of the normal element, σ_J is the total cross section in cm^2 , $S(E)$ is the stopping power in $\text{MeV cm}^2/\text{mg}$, and E_i is the incident projectile energy. The stopping power values used in this work were taken from Northcliffe and Schilling.¹⁸

We have chosen to compare experimental and theoretical yield ratios $R(J/J-2) \equiv Y_J/Y_{J-2}$ for several reasons. First, only the shape of $S(E)$ as

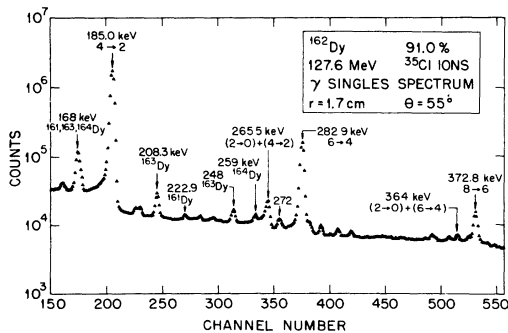


FIG. 1. Ge(Li)-detector spectrum of γ rays resulting from Coulomb excitation of a ^{162}Dy target with ^{35}Cl ions.

a function of E and not the magnitude of $S(E)$ enters into the ratio. Second, a given Y_J value varies linearly as the product of $B(E2; J-2 \rightarrow J)$ and the $B(E2)$'s for all preceding excitation steps in the rotational sequence. However, the ratio $R(J/J-2)$ depends primarily on $B(E2; J-2 \rightarrow J)$, not on lower-spin $B(E2)$ values. Thus a yield ratio is more sensitive to a particular transition rate than is a yield Y_J . Third, the $R(J/J-2)_{\text{exp}}$ values depend only on the relative efficiency of the Ge(Li) detector which can be measured with higher precision than can the absolute efficiency.

Column 8 of Table II gives a comparison of our best values for $R(6/4)$ and $R(8/6)$ with the corresponding theoretical ratios based on rotational E_2 matrix elements. Inclusion of vibrational states and the appropriate E_4 matrix elements¹⁹ in the calculations reduces $R(6/4)_{\text{exp}}/R(6/4)_{\text{theory}}$ by 1.9% and $R(8/6)_{\text{exp}}/R(8/6)_{\text{theory}}$ by 2.6%. Thus the experimental ratios $R(6/4)$ and $R(8/6)$ are appreciably smaller than expected on the basis of the rigid-rotor model. These discrepancies will be discussed in a subsequent section.

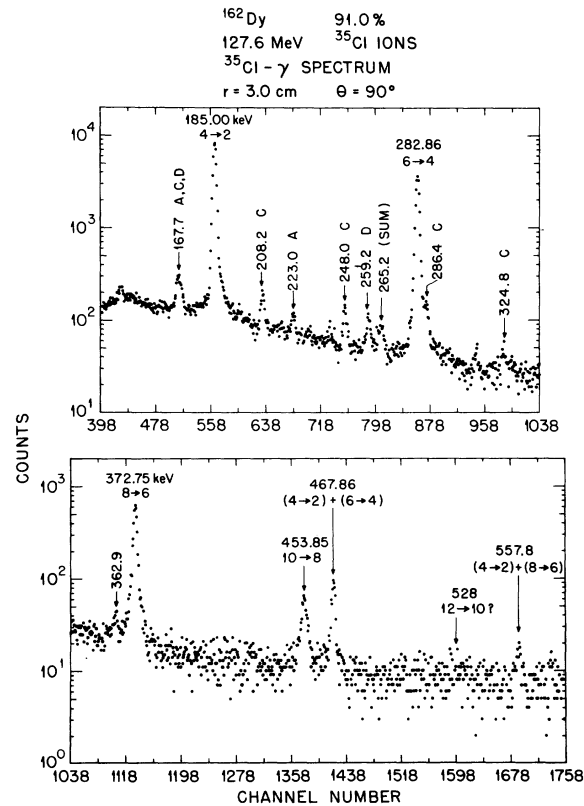


FIG. 2. Ge(Li)-detector spectrum of γ rays in coincidence with ^{35}Cl ions backscattered from a ^{162}Dy target. Peaks labeled A, C, and D are attributed to the isotopic impurities $^{161,163,164}\text{Dy}$, respectively.

TABLE II. Comparison of experimental and theoretical yields of the 4^+ , 6^+ , and 8^+ states in $^{162,164}\text{Dy}$ for Coulomb excitation by ^{35}Cl ions.

Nucleus	$B(E2; 0 \rightarrow 2)^a$	Proj.	E_i (MeV)	J	Experimental	Theoretical	$\left[\frac{R(J/J-2)_{\text{exp}}}{R(J/J-2)_{\text{theory}}} \right]^c$
					yield (10^5 exc/ μC)	yield ^b (10^5 exc/ μC)	
^{162}Dy	5.128	^{35}Cl	127.6	4	242.6	234.2	
				6	31.9	34.3	0.901 ± 0.056
				8	3.06	4.19	0.809 ± 0.051
^{164}Dy	5.403	^{35}Cl	127.6	4	287.6	(287.6)	
				6	37.5	44.6	0.844 ± 0.054
				8	3.71	5.95	0.743 ± 0.059

^a Value used in the theoretical calculation.

^b Theoretical yields were calculated with the Winther-de Boer computer code using rotational model $E2$ matrix elements.

^c $R(6/4) \equiv (6^+ \text{ yield})/(4^+ \text{ yield})$. The errors quoted do not include errors in the $B(E2; 0 \rightarrow 2)$ values.

B. Particle- γ coincident measurements

Gamma rays were observed in coincidence with backscattered projectiles to favor the close collisions which enhance the population of high-spin states. Examples of HI- γ coincident spectra, each of which corresponds to approximately 3×10^7 backscattered ^{35}Cl ions, are shown in Figs. 2 and 3. The γ ray from the $10 \rightarrow 8$ transition can be seen clearly in each spectrum, but the $12 \rightarrow 10$ transitions are scarcely noticeable above background. Guided by the VMI predictions and the known energy⁹ of the $12 \rightarrow 10$ γ ray in ^{160}Dy we find a positive area for each of the weak $12 \rightarrow 10$ γ rays.

A detailed description of the procedure used to determine the experimental Coulomb excitation probabilities has been given elsewhere.⁴ The formula for $(P_J)_{\text{exp}}$ is

$$(P_J)_{\text{exp}} = \frac{1}{N_B a} \left[\frac{(1 + \alpha_T)N}{\bar{W}(\theta)T_\gamma \epsilon} - T_c \right], \quad (2)$$

where N_B is the number of particles that strike the annular counter with sufficient energy to pass a cutoff discriminator and a is the fractional isotopic abundance. α_T is the total conversion coefficient, N is the area of the full-energy peak, $\bar{W}(\theta)$ is a

γ -ray angular distribution factor, T_γ is a γ -ray absorption factor, ϵ is the γ -ray detector efficiency, and T_c is a cascade feeding correction.

The $\bar{W}(\theta)$ factor that appears in Eq. (2) was appreciably different from unity for data taken at 0 and 90° . To check the calculated angular distributions we measured particle- γ angular anisotropies for ^{35}Cl on ^{162}Dy for the strong transitions. In Table III the experimental values are seen to be in good agreement with results of Winther-de Boer calculations. We conclude that, for our thick-target experiments, possible attenuation of the γ -ray angular distributions is so small that the effect on our extracted $B(E2)$ values is negligible. It should be emphasized that the ratio $R(J/J-2) \equiv P_J/P_{J-2}$ depends on the ratio of $\bar{W}(\theta)$ for one transition to $\bar{W}(\theta)$ for the other transition.

For reasons discussed in the previous subsection we have chosen to consider the ratios $R(J/J-2)_{\text{exp}}$, and these are compared with Winther-de Boer calculations based on rigid-rotor $E2$ matrix elements in Table IV. The uncertainties quoted in Table IV include only our experimental uncertainties and not uncertainties inherent in the theoretical calculations. The main contribution to the uncertainties in $R(6/4)_{\text{exp}}$ and $R(8/6)_{\text{exp}}$ is the error in the relative efficiency of the γ -ray detector while statisti-

TABLE III. Particle- γ coincident angular distributions for ^{35}Cl ions on ^{162}Dy : $\bar{W}(\theta) = 1 + g_2 A_2 P_2 + g_4 A_4 P_4$. A_2 and A_4 were calculated with the Winther-de Boer computer code using rotational $E2$ matrix elements. The average laboratory angle for the particle detector was 168.8° , and the γ -ray detector was 6 cm from the target.

Transition	E_γ (keV)	$[\bar{W}(0)/\bar{W}(90)]_{\text{exp}}$	g_2	g_4	$\bar{W}(0)$	$\bar{W}(90)$	$[\bar{W}(0)/\bar{W}(90)]_{\text{theory}}$
4 \rightarrow 2	185	1.796 ± 0.071	0.9418	0.8143	1.208	0.683	1.767
6 \rightarrow 4	283	1.754 ± 0.087	0.9465	0.8289	1.234	0.705	1.750
8 \rightarrow 6	372	1.812 ± 0.189	0.9482	0.8341	1.243	0.740	1.680

TABLE IV. Summary of Coulomb excitation probability ratios obtained from $^{20}\text{Ne}-\gamma$ and $^{35}\text{Cl}-\gamma$ coincident measurements. $R(J/J-2) \equiv P_J/P_{J-2}$.

Nucleus	Proj.	E_i (MeV)	$E_{\text{cut}}(0)$ (MeV)	θ_γ (deg)	$10^2 \times \text{experiment}$				(Experiment/theory) ^{a-c}			
					$R(6/4)$	$R(8/6)$	$R(10/8)$	$R(12/10)$	$R(6/4)$	$R(8/6)$	$R(10/8)$	$R(12/10)$
^{160}Dy	^{35}Cl	127.6	109.0	90	44.89	22.18	16.80	7.4	0.761 ± 0.033	0.926 ± 0.046	1.33 ± 0.16	0.99 ± 0.80
		125.7	105.8	90	42.73	22.01	15.40	12.5	0.808 ± 0.030	1.012 ± 0.049	1.33 ± 0.17	1.81 ± 0.92
^{162}Dy	^{20}Ne	72.8	55.9	0	15.22	6.31	1.001 ± 0.065	0.799 ± 0.067
		^{35}Cl	124.7	102.2	90	44.90	22.13	12.33	...	0.888 ± 0.056	1.042 ± 0.080	1.09 ± 0.28
	^{35}Cl	127.6	108.7	55	49.81	20.91	21.45	...	0.787 ± 0.040	0.832 ± 0.055	1.52 ± 0.25	...
	^{35}Cl	127.6	108.7	90	50.71	22.19	13.62	13.5	0.809 ± 0.033	0.867 ± 0.032	1.07 ± 0.11	1.78 ± 0.67
^{164}Dy	^{20}Ne	125.7	105.5	90	50.17	20.75	22.89	...	0.897 ± 0.051	0.910 ± 0.090	1.78 ± 0.54	...
		72.8	55.8	0	16.51	8.10	0.980 ± 0.073	0.926 ± 0.072
	^{35}Cl	124.7	101.9	90	55.81	21.93	13.30	...	0.975 ± 0.072	0.917 ± 0.065	0.98 ± 0.15	...
		127.6	108.4	55	54.36	20.83	22.98	...	0.754 ± 0.050	0.734 ± 0.046	1.42 ± 0.21	...
		127.6	108.4	90	59.71	23.23	15.07	10.8	0.835 ± 0.039	0.833 ± 0.036	1.01 ± 0.11	1.25 ± 0.62

^a The $B(E2; 0 \rightarrow 2)$ values used in the calculations were 5.057, 5.128, and 5.403 $e^2 10^{-48} \text{ cm}^4$ for $^{160,162,164}\text{Dy}$, respectively.

^b Theoretical values were calculated with the Winther-de Boer computer code using rotational $E2$ matrix elements.

^c Errors quoted do not include errors in the theoretical $R(J/I)$ values.

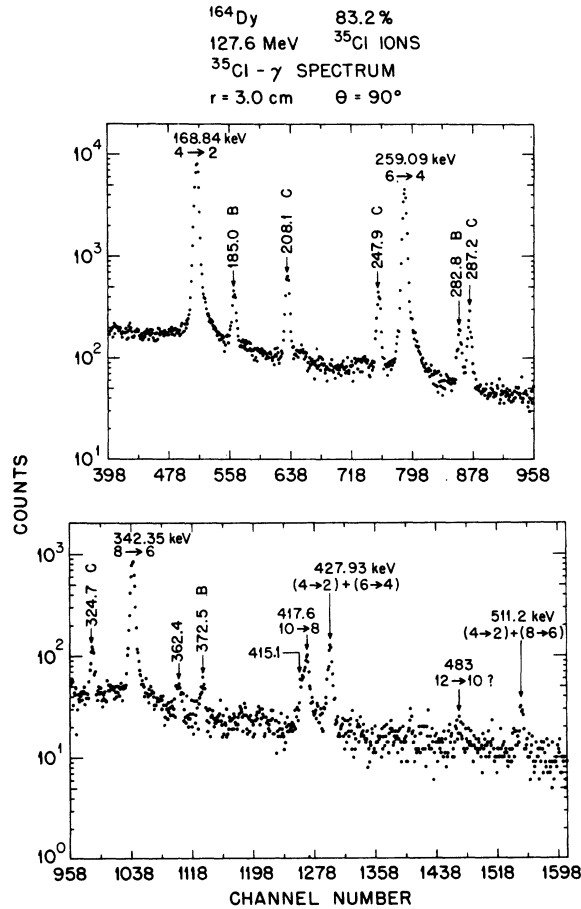


FIG. 3. Ge(Li)-detector spectrum of γ rays in coincidence with ^{35}Cl ions backscattered from a ^{164}Dy target. Peaks labeled A, B, and C are attributed to the isotopic impurities $^{161,162,163}\text{Dy}$, respectively.

cal uncertainties are predominant for $R(10/8)_{\text{exp}}$ and $R(12/10)_{\text{exp}}$.

In column 4 of Table V we compare our best values for the $R(J/J-2)$ ratios from particle- γ coincident measurements to those based on rotational $E2$ calculations. These best values are weighted averages of the values in columns 10-13 of Table IV. For $^{162,164}\text{Dy}$ the 6/4 and 8/6 ratios in Table V are in good agreement with the corresponding ratios from γ -ray yield measurements shown in column 8 of Table II. Columns 5 and 6 of Table V will be discussed in a subsequent paragraph.

Before $B(E2)$ values were extracted from our experimental probability ratios the theoretical calculations were modified to account for the effects of vibrational states, $E4$ Coulomb excitation, and quantum corrections. The magnitudes of these effects are indicated in Table VI for a representative case, 125.7-MeV ^{35}Cl ions on ^{162}Dy .

The results in Table VI are given relative to a Winther-de Boer calculation with rotational $E2$ matrix elements for the ground band up through spin 12. Columns 2 and 5 refer to an 18-state calculation including even-spin states in the $K^\pi = 2^+$ γ -vibrational band and odd-spin states in the $K^\pi = 2^-$ octupole-vibrational band up through spin 12. The relevant $E2$ matrix elements were obtained from $B(E2)$ values and branching ratios where known²⁰ and from the rotational model otherwise. The change in each $R(J/J-2)_{\text{theory}}$ value due to inclusion of vibrational states is less than the experimental uncertainty in the corresponding $R(J/J-2)_{\text{exp}}$ value. Separate computations showed that the effects on the ground-band probabilities of the odd-spin members of the γ band and the even-spin members of the octupole band are negligible. Fi-

TABLE V. Summary of best values for double probability ratios from particle- γ coincident data and best $B(E2)$ values.

Nucleus	$B(E2; 0 \rightarrow 2)^a$ ($e^2 10^{-48} \text{ cm}^4$)	J/I	$\left[\frac{R(J/I)_{\text{exp}}}{R(J/I)_{\text{theory}}} \right]^b$	$B(E2; I \rightarrow J)^c$ ($e^2 10^{-48} \text{ cm}^4$)	$\left[\frac{B(E2; I \rightarrow J)}{B(E2; I \rightarrow J_{\text{rot}})} \right]^d$
^{160}Dy	5.057	4/2		2.50 ± 0.25	0.96 ± 0.10
		6/4	0.788 ± 0.023	1.78 ± 0.09	0.77 ± 0.05
		8/6	0.970 ± 0.042	2.05 ± 0.13	0.94 ± 0.06
		10/8	1.334 ± 0.116	2.73 ± 0.27	1.29 ± 0.14
		12/10	1.58 ± 0.68	3.17 ± 1.37	1.53 ± 0.66
^{162}Dy	5.128	4/2		2.64 ± 0.24	1.00 ± 0.09
		6/4	0.856 ± 0.036	2.00 ± 0.09	0.86 ± 0.05
		8/6	0.879 ± 0.027	1.85 ± 0.10	0.84 ± 0.05
		10/8	1.221 ± 0.159	2.53 ± 0.34	1.18 ± 0.16
		12/10	1.78 ± 0.67	3.62 ± 1.39	1.72 ± 0.66
^{164}Dy	5.403	4/2		2.83 ± 0.31	1.02 ± 0.11
		6/4	0.866 ± 0.051	2.06 ± 0.11	0.84 ± 0.05
		8/6	0.839 ± 0.032	1.86 ± 0.11	0.80 ± 0.05
		10/8	1.110 ± 0.131	2.44 ± 0.32	1.08 ± 0.14
		12/10	1.25 ± 0.62	2.68 ± 1.35	1.21 ± 0.61

^a Value used in theoretical calculations. See Ref. 22.

^b Theoretical values were calculated with the Winther-de Boer computer code using rotational $E2$ matrix elements. Errors quoted do not include errors in the theoretical $R(J/I)$ values.

^c Theoretical uncertainties are included in the quoted errors. Singles data (see Table II) and particle- γ data were used to determine $B(E2; 4 \rightarrow 6)$ and $B(E2; 6 \rightarrow 8)$ values for $^{162,164}\text{Dy}$.

^d Quoted errors include error in $B(E2; 0 \rightarrow 2)$.

nally, it should be pointed out that the $R(J/J-2)$ are rather insensitive to changes in sign of the ground- γ band matrix elements.

Columns 3 and 6 in Table VI reflect the effect of including rotational model $E4$ matrix elements based on the $B(E4; 0 \rightarrow 4)$ value of Erb *et al.*¹⁹ The change in $R(12/10)$ is only half the change in P_{12} .

A full quantum-mechanical coupled-channels code for high spins is sorely needed to remove a possible ambiguity in $B(E2)$ values extracted from multiple Coulomb excitation data. Recently, how-

TABLE VI. Estimates of changes in ground-band P_J and $R(J/J-2)$ values due to inclusion of vibrational states, $E4$ Coulomb excitation, and quantal corrections for the case of 125.7-105.7-MeV ^{35}Cl ions on ^{162}Dy . See text for discussion of calculations.

J	Percent change in P_J			Percent change in $R(J/J-2)$		
	Vib.	$E4$	Quantal	Vib.	$E4$	Quantal
4	-3.0	-2.9	-1. ^a			
6	-0.5	-0.6	-4. ^a	2.6	2.4	-3. ^a
8	2.2	3.5	-8. ^a	2.8	4.1	-4. ^a
10	6.2	9.1	(-14.) ^b	3.9	5.3	(-6.) ^b
12	7.8	20.3	(-22.) ^b	1.5	10.2	(-8.) ^b

^a Value obtained by $1/\eta$ extrapolation of calculated values from Ref. 21.

^b Rough extrapolation from results for lower-spin states.

ever, Alder²¹ has calculated quantal corrections for a 0, 2, 4, 6, 8 rotational band for $\eta = Z_1 Z_2 e^2 / \hbar v = 10, 15,$ and 20 . We assumed a $1/\eta$ dependence and extrapolated to zero quantal correction for $\eta = \infty$ to obtain corrections for our η value of 100. These are given in Table VI with our crude estimates for spins 10 and 12. Our method of considering probability ratios produces cancellation of a significant part of the quantal correction. We have included uncertainties of 1, 2, 3, and 4% in the theoretical 6/4, 8/6, 10/8, and 12/10 ratios, respectively, although confirmation of the validity of the latter two assignments must await a full coupled-channels calculation.

Another potential uncertainty in $R(J/I)_{\text{theory}}$ arises from possible nonrotational static quadrupole moments Q_J . Fortunately the P_J are not highly sensitive to the values of Q_J . For example setting Q_{10} equal to zero instead of the rigid-rotor value increases P_{10} by only 18%. We typically assigned uncertainties of 2% to $R(J/I)_{\text{theory}}$ to account for possible nonrotational Q_J behavior.

Our best $B(E2)$ values are given in column five of Table V. The $B(E2; 2 \rightarrow 4)$ values were obtained from ^{35}Cl - γ measurements for which absolute values of $(P_4)_{\text{exp}}$ were determined. For $^{162,164}\text{Dy}$ the $B(E2; 4 \rightarrow 6)$ and $B(E2; 6 \rightarrow 8)$ values represent a weighted average of values from γ -ray singles and particle- γ coincident measurements. The formula

for the $B(E2)$ values,

$$B(E2; I \rightarrow J) = C^2(I \ 2J; 00)B(E2; 0 \rightarrow 2) \\ \times R(J/I)_{\text{exp}}/R(J/I)_{\text{theory}}, \quad (3)$$

gave results consistent with those obtained by adjusting matrix elements in the computations to produce agreement with experiment.

We note that the $B(E2)$ values obtained here are not sensitive to the $B(E2; 0 \rightarrow 2)$ value chosen for the Winther-de Boer code. Of course the ratios of $B(E2; I \rightarrow J)$ to the rigid-rotor values, given in column 6 of Table V, depend on $B(E2; 0 \rightarrow 2)$. We assigned uncertainties of $\pm 3\%$ to $B(E2; 0 \rightarrow 2)$ since the recent Pittsburgh values¹⁹ for $^{162,164}\text{Dy}$ are significantly larger than those of Löbner, Vetter, and Hönig²² which were used to derive the results in column 6. Adoption of the Pittsburgh $B(E2; 0 \rightarrow 2)$ values would reduce the ratios in column 6 by 5% for ^{162}Dy and 3% for ^{164}Dy .

IV. DISCUSSION AND CONCLUSIONS

We have extracted $B(E2)$ values between states up through spin 12 in the ground bands of three even Dy nuclides by means of multiple Coulomb excitation measurements. The $B(E2; 2 \rightarrow 4)$ were determined to accuracies of 10%, $B(E2; 4 \rightarrow 6)$ and $B(E2; 6 \rightarrow 8)$ to 6%, $B(E2; 8 \rightarrow 10)$ to 13%, and $B(E2; 10 \rightarrow 12)$ to about 40%.

Within uncertainties the $B(E2; 2 \rightarrow 4)$ are consistent with rigid-rotor predictions. For $^{162,164}\text{Dy}$ the $B(E2; 4 \rightarrow 6)$ and $B(E2; 6 \rightarrow 8)$ values are significantly smaller and the $B(E2; 8 \rightarrow 10)$ values are slightly larger than expected from the pure rotational model. The most striking variation of $B(E2)$ with spin occurs for ^{160}Dy , with the $10 \rightarrow 8$ transition being appreciably faster than rotational. A quantal correction that is larger than our estimate of 6%

would increase the discrepancy between experiment and rigid-rotor predictions for the $10 \rightarrow 8$ transitions.

In Fig. 4 the results of Table V are displayed graphically along with recent Notre Dame²⁰ results from Coulomb excitation with ^{16}O ions. There is excellent agreement between the two sets of data for the $2 \rightarrow 4$ and $4 \rightarrow 6$ transitions. Although the Notre Dame values for the $6 \rightarrow 8$ transitions are systematically larger than our values, the disagreement is not serious when experimental uncertainties are considered.

A very recent determination²³ of lifetimes in ^{160}Dy by the Doppler-shift attenuation method (DSAM) yielded $B(E2; 6 \rightarrow 8)$ and $B(E2; 10 \rightarrow 12)$ values that agree with our multiple Coulomb excitation (MCEX) measurements. However the DSAM $B(E2)$ value for the $4 \rightarrow 6$ transition is 30% larger and that for the $8 \rightarrow 10$ transition is 30% smaller than the corresponding MCEX values. A serious difficulty with DSAM lifetimes is due to imperfect knowledge of the stopping power $S(E)$. Recently Sie *et al.*²⁴ found it necessary to increase the $S(E)$ of Northcliffe and Schilling¹⁸ by 20% to make their DSAM lifetimes for ^{152}Sm and ^{156}Gd agree with recoil-distance lifetimes.⁶ Possibly the DSAM lifetime of the 6^+ state in ^{160}Dy could be scaled up enough to be consistent with the MCEX result; however this scaling would destroy the agreement for the 8^+ state and widen the disagreement for the 10^+ state. At the present time the basis for this discrepancy between DSAM and MCEX lifetimes is not clear.

Our anomalous $B(E2; 4 \rightarrow 6)$ and $B(E2; 6 \rightarrow 8)$ values could be a consequence of: (1) a systematic experimental effect, (2) an inadequate theoretical treatment of multiple Coulomb excitation, or (3) incorrect estimates of the perturbing influences of static moments, $E4$ Coulomb excitation, vibrational states, etc. A major experimental error is unlikely for $B(E2; 4 \rightarrow 6)$ because our results are strongly corroborated by Oehlberg *et al.*²⁰ who used thin targets and a different projectile. We expect Coulomb excitation theory to be applicable if quantal corrections are made properly and if Coulomb-nuclear interference is not serious. A quantal correction of 15% to $R(\frac{2}{3})$ has been calculated²¹ for $\eta = 20$ and a $1/\eta$ extrapolation gives only a 3% correction for $\eta = 100$. In the α -particle bombardment of rare-earth nuclei Bemis *et al.*²⁵ recently observed small departures from pure Coulomb excitation at incident energies that correspond to a separation distance between surfaces, Δ , of 8 fm if spherical surfaces with radii of $1.2A^{1/3}$ fm are assumed. For ^{166}Er the deviations were 1–2% for the 2^+ state and about 5% for the 4^+ state for $\Delta = 6$ fm. However, Christensen *et al.*²⁶ found vir-

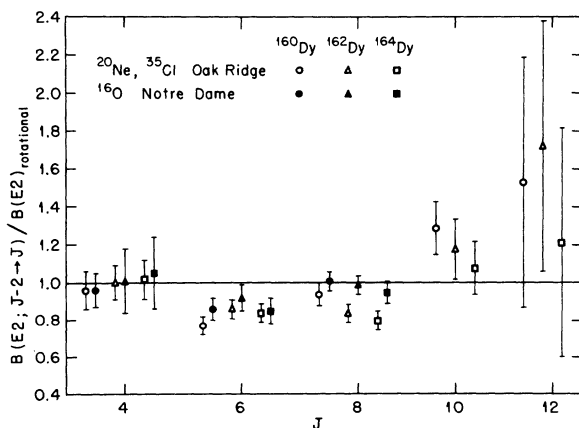


FIG. 4. Comparison of $B(E2)$ values derived from Coulomb excitation measurements with rigid-rotor predictions.

tually no Coulomb-nuclear interference in the excitation of the 2^+ state in ^{58}Ni by ^{16}O ions scattering at backward angles for separation distances larger than 5.3 fm. Furthermore, in the case of excitation of the 2^+ state by backscattered projectiles, the interference minimum occurs at $\Delta \approx 3.8$ fm for α particles²⁵ and at $\Delta \approx 2.9$ fm for ^{16}O ions.²⁶ Thus for a given separation and depth of minimum, Coulomb-nuclear interference is probably less important with heavy-ion projectiles than with α particles. We believe that the present experimental accuracy of 6% for $R(\frac{6}{4})$ does not require such stringent "safe" bombarding conditions as those needed for reorientation experiments²⁷ with heavy ions. In our thick-target experiments with ^{35}Cl ions the projectile incident energy range was typically 126 to 106 MeV. To check for Coulomb-nuclear interference effects we set a narrow digital window, 127.6 to 120.9 MeV, as well as a wide digital window, 127.6 to 108.7 MeV, on the heavy-ion energy for one of the ^{35}Cl - γ runs. The narrow window corresponded to $\Delta = 5.0$ -5.8 fm, and the wide window to $\Delta = 5.0$ -7.7 fm. We found $R(6/4)_{\text{exp}}/R(6/4)_{\text{theory}}$ to be 0.811 for the narrow window and 0.801 for the wide window. In addition, the singles measurements, where the range of Δ was 5.0 fm to essentially infinity, gave $R(6/4)$ values that agree well with those from the particle- γ coincident data. Hence we doubt that Coulomb-nuclear interference is significant in the present work. There is a clear need, however, for experimental information on Coulomb-nuclear interference for 6^+ and higher-spin states.

Concerning effect (3), we calculated the magnitudes of perturbing influences needed to produce agreement between $R(6/4)_{\text{exp}}$ and $R(6/4)_{\text{theory}}$. These

are: (a) a static electric quadrupole moment for the 6^+ state, Q_0 , that is 40% larger than the rigid-rotor value; (b) a value $\langle 0||M(E4)||4\rangle = -1.3$ which implies a hexadecapole deformation, β_{40} , of -0.47 , whereas theory²⁸ and experiment¹⁹ indicate that β_{40} is positive for the Dy nuclei; (c) high-lying $K=4$ bands strongly coupled to the ground band with judicious sign choices for the interband matrix elements. We think it highly unlikely that (a), (b), or (c) is the explanation although some combination such as $Q_0 = 1.2Q_{\text{rot}}$ and weak couplings of many unobserved higher-lying levels cannot now be ruled out. For the discussion which follows, we assume that no important effect was overlooked in our determination of experimental and theoretical $R(J/I)$ values.

Two surprising trends can be seen in Fig. 4. One is the 10-15% dip in $B(E2; 4-6)$ below the rotational prediction, and the other is a jump in $B(E2)$ at the 10^+ state. If other perturbing factors are ignored, centrifugal stretching is implied by the $B(E2; 8-10)$ values while the dip in $B(E2; 4-6)$ could be explained only by a large reduction in the nuclear deformation, i.e., shrinking. The present data suggest that other perturbing factors must exert an important influence on the $B(E2)$ values in the ground bands of $^{160,162,164}\text{Dy}$.

Recently Kumar²⁹ used the pairing-plus-quadrupole model to calculate transition rates between levels in ^{160}Dy . His results show a gradual increase in $B(E2)$ values up to spin 16 and hence do not agree with the present data.

In an attempt to gain further insight into the observed deviations from rotational behavior, we have analyzed our data in terms of a purely phenomenological expansion in powers of the angular

momentum. We choose the expansion

$$\frac{\langle I||M(E2)||J\rangle}{C(I2J;00)(2I+1)^{1/2}} = \langle 0||M(E2)||2\rangle_0 \left[1 + \delta \left\{ \frac{1}{2}[I(I+1) + J(J+1)] \right\}^{1/2} + \frac{\alpha}{2}[I(I+1) + J(J+1)] + \dots \right], \quad (4)$$

where $\langle 0||M(E2)||2\rangle_0$ is the unperturbed matrix element and where we keep only the first three terms. The definition of the reduced matrix element is

$$\langle I||M(E2)||J\rangle = \pm [(2I+1)B(E2; I-J)]^{1/2} \quad (5)$$

and the rigid-rotor prediction is

$$\langle I||M(E2)||J\rangle_{\text{rot}} = (-1)^{I-J} (2I+1)^{1/2} C(I2J;00) \times \langle 0||M(E2)||2\rangle. \quad (6)$$

Except for the δ term our expansion is similar to that of Diamond *et al.*² which is based on the for-

mulas of Symons and Douglas.³⁰ These formulas come out of the usual treatment in which the $K=0$ and $K=2$ vibrational bands are mixed with the ground band. Our δ term embodies a possible functional dependence for perturbing effects other than centrifugal stretching. We wish to emphasize, however, the highly empirical nature of the δ term.

In Fig. 5 the left side of Eq. (4) is plotted as a function of $\frac{1}{2}[I(I+1) + J(J+1)]$ for ^{160}Dy . A horizontal line on this graph would represent the rotational limit, and the usual stretching formulation would give a straight line whose intercept would be

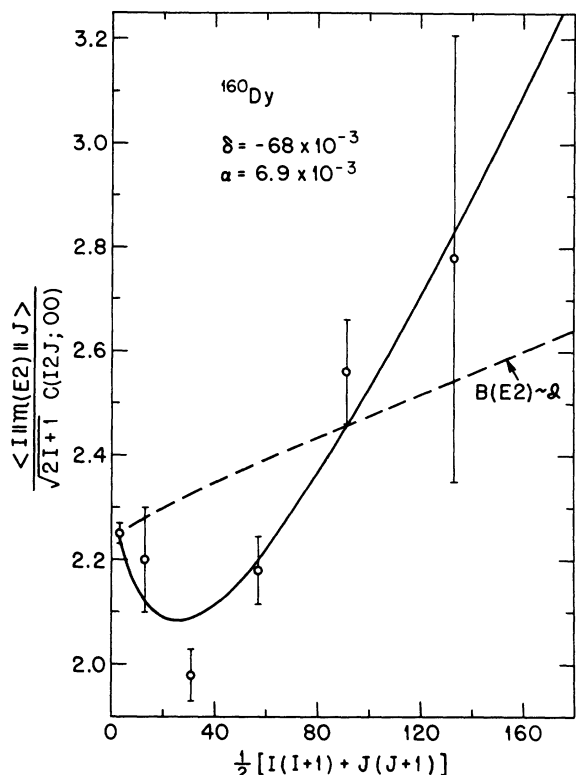


FIG. 5. Plot of $\langle I || M(E2) || J \rangle / C(I2J; 00) \sqrt{2I+1}$ as a function of $\frac{1}{2} [I(I+1) + J(J+1)]$. The solid line is a least-square fit of Eq. (4) to the five data points, and the dashed line was derived from the assumption $B(E2) \sim \mathcal{J}$.

the unperturbed value $\langle 0 || M(E2) || 2 \rangle_0$. A straight line cannot be fit to the data, and we conclude that the stretching approximation is poor.

Since the moment of inertia presumably reflects the influence of all perturbations on the level en-

ergies, we depict in Fig. 5 the curve that results from the assumption $B(E2) \sim \mathcal{J}$. Clearly this assumption is not consistent with our data. Also displayed is the result of an unweighted least squares fit of expansion (4) to the data. The fit is superior to the $B(E2) \sim \mathcal{J}$ curve as might be expected since an additional parameter is involved, but a troublesome point is that the fit requires large values of δ and α . We find $10^3\delta = -68, -76, -59$, and $10^3\alpha = 6.9, 7.4, 5.1$, for $^{160,162,164}\text{Dy}$, respectively. These α values are 5 times larger than those predicted from energy-level B/A values on the basis of centrifugal stretching. Furthermore the empirical δ term is sizable even for spin 2 and thus $\langle 0 || M(E2) || 2 \rangle_0 \approx 1.1 \langle 0 || M(E2) || 2 \rangle$. Most importantly, the physical basis for the δ term is not clear. If one assumes there is $\Delta K = 1$ Coriolis mixing, then unreasonably large admixed amplitudes in the ground-band wave functions are required because no low-lying bands with $K = 1$ are known to exist in the even Dy nuclei.

One conclusion that can be drawn from Fig. 5 is that still greater experimental accuracy for low spins and measurements at higher spins are needed to understand the observed deviations from rotational behavior.

ACKNOWLEDGMENTS

We are indebted to Dr. G. B. Hagemann and Dr. F. K. McGowan for helpful discussions and to E. D. Hudson and M. L. Mallory for development of the ^{35}Cl beam. One of us (ROS) gratefully acknowledges partial support under National Science Foundation CoSIP Grant No. GY7120 and under a Research Corporation Cottrell College Science Grant.

*Work sponsored by the U. S. Atomic Energy Commission under contract with Union Carbide Corporation.

¹M. A. J. Mariscotti, G. Scharff-Goldhaber, and B. Buck, Phys. Rev. **178**, 1864 (1969).

²See R. M. Diamond, G. D. Symons, J. L. Quebert, K. H. Maier, J. R. Leigh, and F. S. Stephens, Nucl. Phys. **A184**, 481 (1972), and Refs. 2-17 therein.

³J. de Boer, G. Goldring, and H. Winkler, Phys. Rev. **134**, B1032 (1964).

⁴R. O. Sayer, P. H. Stelson, F. K. McGowan, W. T. Milner, and R. L. Robinson, Phys. Rev. C **1**, 1525 (1970).

⁵L. L. Riedinger, G. Schilling, A. E. Rainis, R. N. Oehlberg, E. G. Funk, and J. W. Mihelich, Bull. Am. Phys. Soc. **17**, 537 (1972).

⁶D. Ward, R. L. Graham, J. S. Geiger, N. Rud, and A. Christy, Nucl. Phys. **A196**, 9 (1972).

⁷R. M. Diamond, F. S. Stephens, W. H. Kelly, and

D. Ward, Phys. Rev. Lett. **22**, 546 (1969).

⁸See also R. O. Sayer, E. Eichler, N. R. Johnson, and D. C. Hensley, Bull. Am. Phys. Soc. **17**, 28 (1972).

⁹A. Johnson, H. Ryde, and S. A. Hjorth, Nucl. Phys. **A179**, 753 (1972).

¹⁰R. Gunnick, J. B. Niday, R. P. Anderson, and R. A. Meyer, Lawrence Livermore Laboratory Report No. UCID-15439, 1969 (unpublished).

¹¹L. J. Jardine, Nucl. Instrum. Methods **96**, 259 (1971).

¹²The α_T values were obtained from the tables of L. A. Sliv and I. M. Band, *Internal Conversion Coefficients* (North-Holland, Amsterdam, 1958).

¹³G. B. Hagemann, D. C. Hensley, N. R. Johnson, W. T. Milner, and L. L. Riedinger, Bull. Am. Phys. Soc. **18**, 581 (1973).

¹⁴G. E. Keller and E. F. Zganjar, Nucl. Phys. **A147**, 527 (1970).

¹⁵A. Bäcklin, A. Suarez, O. W. B. Schult, B. P. K.

- Maier, U. Gruber, E. B. Shera, D. W. Hafemeister, W. N. Shelton, and R. K. Sheline, *Phys. Rev.* 160, 1011 (1967).
- ¹⁶O. W. B. Schult, U. Gruber, B. P. Maier, and F. W. Stanek, *Z. Physik* 180, 298 (1964).
- ¹⁷A. Holm, private communication.
- ¹⁸L. C. Northcliffe and R. F. Schilling, *Nucl. Data* A7, 233 (1970).
- ¹⁹K. A. Erb, J. E. Holden, I. Y. Lee, J. X. Saladin, and T. K. Saylor, *Phys. Rev. Lett.* 29, 1010 (1972).
- ²⁰R. N. Oehlberg, L. L. Riedinger, A. E. Rainis, A. G. Schmidt, E. G. Funk, and J. W. Mihelich, to be published.
- ²¹K. Alder, private communication.
- ²²K. E. G. Löbner, M. Vetter, and V. Hönig, *Nucl. Data* A7, 495 (1970).
- ²³G. B. Hagemann, D. C. Hensley, W. T. Milner, E. Eichler, N. R. Johnson, L. L. Riedinger, and R. O. Sayer, to be published.
- ²⁴S. H. Sie, D. Ward, R. L. Graham, J. S. Geiger, and H. R. Andrews, *Bull. Am. Phys. Soc.* 18, 629 (1973).
- ²⁵C. E. Bemis, Jr., P. H. Stelson, F. K. McGowan, W. T. Milner, J. L. C. Ford, Jr., R. L. Robinson, and W. Tuttle, *Phys. Rev. C* 8, 1934 (1973).
- ²⁶P. R. Christensen, I. Chernov, E. E. Gross, R. Stokstad, and F. Videbaek, *Nucl. Phys.* A207, 433 (1973).
- ²⁷D. Cline, H. S. Gertzman, H. E. Gove, P. M. S. Lesser, and J. J. Schwartz, *Nucl. Phys.* A133, 445 (1969); J. A. Thomson, R. P. Scharenberg, and W. R. Lutz, *Phys. Rev. C* 4, 1699 (1971).
- ²⁸U. Götze, H. C. Pauli, K. Alder, and K. Junker, *Nucl. Phys.* A192, 1 (1972).
- ²⁹K. Kumar, *Phys. Rev. Lett.* 30, 1227 (1973).
- ³⁰G. D. Symons and A. C. Douglas, *Phys. Lett.* 24B, 11 (1967).